NASA CR-72530

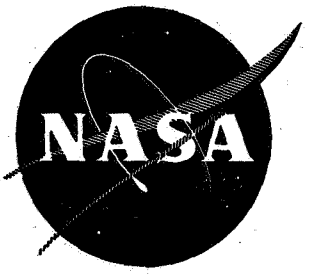

STUDY OF ROLLING-CONTACT PHENOMENA IN MAGNESIUM OXIDE

by

K. F. Dufrane and W. A. Glaeser

prepared for

NATIONAL AERONAUTICS AND SPACE ADMINISTRATION

Contract NAS 3-6263

BATTELLE MEMORIAL INSTITUTE
Columbus Laboratories

SECOND SUMMARY REPORT

on

STUDY OF ROLLING-CONTACT PHENOMENA IN MAGNESIUM OXIDE

by

K. F. Dufrane and W. A. Glaeser

prepared for

NATIONAL AERONAUTICS AND SPACE ADMINISTRATION

April 14, 1969

Contract NAS 3-6263, Task Order No. 5

Technical Management
NASA Lewis Research Center
Cleveland, Ohio
D. P. Townsend, Project Manager
E. V. Zaretsky, Research Advisor

BATTELLE MEMORIAL INSTITUTE
Columbus Laboratories
505 King Avenue
Columbus, Ohio 43201

ABSTRACT

Basic phenomena associated with rolling-contact deformation were studied in MgO single crystals deformed by a rolling hardened steel ball to avoid the complications of inclusions, grain boundaries, and multiple phases existing in normal bearing alloys. Examination of thin films from the rolling-contact tracks by transmission electron microscopy revealed that changes in dislocation density and interaction were responsible for measured variations in track width and hardness. The presence of adsorbed toluene on the surface caused a change in slip mode and premature spalling similar to previous results with oil. The effect of adsorbed fluids on slip mode is probably caused by their influence on dislocation mobility. High-speed elastohydrodynamic rolling produced slip in narrow bands across the contact track, which is caused by the initiation of dislocations only at subsurface sites. Continued rolling caused the bands to widen and eventually cover the entire track width. The cause for fatigue spalls in MgO may be related to fatigue failures in real bearing materials. Further studies with MgO and more complicated model bearing materials are recommended.

TABLE OF CONTENTS

	Page
INTRODUCTION	1 1
SUMMARY	2
EXPERIMENTAL METHOD	2
Crystal Preparation	2
Apparatus	3
Materials Properties	3
ROLLING-CONTACT SLIP CHARACTERISTICS	3
EXPERIMENTAL RESULTS AND DISCUSSION	5
Reciprocating Rolling	5
Track Hardness	5
Thin-Film Electron Microscopy	9
Depth of Dislocation Penetration	14
Adsorbed Fluids	15
Elastohydrodynamic Rolling	19
Film-Thickness Calculations	19
Track Characteristics	20
Track-Width and Hardness Measurements	20
Elastohydrodynamic Slip Characteristics	24
CONCLUSIONS	25
RECOMMENDED FUTURE STUDIES	26
REFERENCES	27

STUDY OF ROLLING-CONTACT PHENOMENA IN MAGNESIUM OXIDE

by

K. F. Dufrane and W. A. Glaeser

INTRODUCTION

Fatigue failure of rolling-element bearings continues to be the limiting factor of bearing life in spite of recent materials and lubricant improvements. The unpredictable nature of fatigue failure prevents reliable design of machine elements that depend critically on rolling-element bearings. Since further improvements of fatigue life will probably result only from a basic understanding of the fatigue mechanism, a study was initiated at Battelle to determine the effect of rolling-contact stress on basic deformation and fatigue mechanisms.

The deformation characteristics of all solids result from the generation, motion, and interaction of dislocations. As the complexity of the solid increases with grain boundaries, multiple phases, and impurity precipitates, the understanding of deformation becomes increasingly difficult. A simple solid with well-established slip systems was therefore considered necessary as a beginning material to study basic rolling-contact deformation and fatigue mechanisms. Single-crystal, high-purity magnesium oxide was found to fulfill the requirements of a simple model bearing material. Its well-established slip systems and experimental convenience permitted simple analysis of deformation from rolling-contact stresses. The approach was to establish the basic deformation processes in magnesium oxide and then progress to more complex bearing materials. As the influence of the complicating factors of grain boundaries, multiple phases, and impurity precipitates on rolling-contact deformation was established, the mechanisms responsible for fatigue failures in rolling-element bearings would be identified.

Early experiments identified the operating slip systems to be those with maximum applied shear stress.[1] Dislocations propagated from sources located beneath the surface near the region of the calculated maximum shear stress. The depth of dislocation penetration was found to be greater on planes of maximum shear stress that were parallel to the rolling direction than on similar planes that were inclined at 45 degrees to the rolling direction. As the number of reciprocating rolling cycles increased, the track width increased, reached a plateau, and then increased again. Spalling, very similar to fatigue spalls seen in actual bearing elements, often occurred during the second increase of the track width.

Recent studies under Task Order No. 4 of Contract NAS 3-6263 revealed several further interesting features.[2] The depth of dislocation propagation decreased at increasing rolling velocities, which could be explained in terms of dislocation dynamics. Measurements of ball and track wear could not explain the variations in track width with rolling-contact cycles. Rolling with a lubricant present under boundary lubrication conditions caused a change in slip mode that led to spalling in 10^3 cycles as opposed to at least 10^5 cycles for dry contact. The lubricant apparently interacted with

the MgO surface to cause this effect. Examination of thin films made in the tracks revealed high dislocation densities and extensive dislocation interaction after only 100 rolling-contact cycles.

The activities under Task Order No. 5 of Contract NAS 3-6263 during the 12 months following July 19, 1967, have been a continuation of the study of rolling-contact phenomena in magnesium oxide.

SUMMARY

Optical-quality MgO single crystals were subjected to rolling-contact deformation by an 0.25-inch-diameter (0.635 cm) hardened AISI 52100 steel ball. The track hardness varied with the number of rolling-contact cycles similar to that of previous track-width measurements. Thin-foil transmission electron microscopy confirmed that changes in dislocation density and interaction caused the measured variations in track width and hardness with repeated application of rolling-contact stress. The depth of dislocation propagation, or slip, was less for higher rolling velocities even after extended numbers of cycles of reciprocating, low-speed rolling. Adsorbed toluene on a water-free MgO surface caused $\{110\}_{90}$ slip and premature spalling similar to that with oil, which indicates the same phenomena occurred with both liquids. Elastohydrodynamic oil films caused slip to be concentrated in narrow bands across the track region. The bands widened with increasing cycles to eventually form a uniform dislocation configuration across the track. The track width and hardness increased more rapidly and reached maximum levels sooner with elastohydrodynamic rolling than with solid surface contact.

EXPERIMENTAL METHOD

Crystal Preparation

MgO crystals of optical quality were purchased from the Norton Company. The bulk crystals, measuring 3/4 x 3/4 x 1/4 inch (1.9 x 1.9 x 0.6 cm), were annealed in air at 1200 C for 24 hours and furnace cooled to facilitate cleaving. A magnesite (industrial MgO) crucible was used as a container to avoid contamination, and no color change occurred during annealing.

Specimens of appropriate size were cleaved from the bulk crystals with a chisel and hammer. Specimens measuring 1/16 x 1/4 x 3/4 inch (0.16 x 0.6 x 1.9 cm) were used for reciprocating rolling experiments, while specimens measuring 1/16 x 3/4 x 3/4 inch (0.16 x 1.9 x 1.9 cm) were used for elastohydrodynamic experiments. Cleavage steps on the surface of the reciprocating rolling specimens were leveled by chemical polishing in orthophosphoric acid at 220 F for 1-minute intervals up to 5 minutes. The surfaces were examined at 50X after each minute to follow the leveling process. The crystal was discarded if cleavage steps or other imperfections remained after 5

minutes of polishing. Since very flat specimens were required to prevent ball skipping in the high-speed elastohydrodynamic experiments, the specimens were ground on a glass plate with 800-grit silicon carbide until all cleavage steps were removed. The specimens were then chemically polished in orthophosphoric acid to remove the surface damage from grinding. The resulting surfaces were very flat without the normal rounded cleavage steps.

Apparatus

A 0.25-inch-diameter (0.635 cm) 52100 steel ball mounted on a shaft held between conical pivot bearings was used in all experiments. A sketch of the ball, shaft, mounting, and crystal is shown in Figure 1. For reciprocating motion (1a), the ball mounting was suspended under a triangular table so that the ball provided one point of a three-point contact configuration. The other two points of contact were nylon feet that slid in a vee way to maintain straight-line ball movement. Ball loading was by dead weights applied to the top of the table. The table was driven by a crank arm on a small electric gear motor, and rolling speed was varied by changing gear motors.

For the elastohydrodynamic experiments (1b), the mounting was fastened eccentrically on a vertical shaft in a drill press. The resulting ball path was circular, with its diameter determined by the amount of eccentricity of the mounting. The load was controlled by counterbalancing the drill-press chuck. Oil was supplied by flooding the specimen.

Materials Properties

The following mechanical properties of MgO and AISI 52100 steel were used, where pertinent, in calculations of contact stresses:

Material	Young's Modulus		Poisson's Ratio	Tensile Yield Strength		Hardness
	10^6 psi	10^4 Kg/mm^2		1000 psi	Kg/mm^2	
MgO	38	2.7	0.25	8 to 9	5.6 to 6.3	370 KHN
AISI 52100 steel	29	2.0	0.3	200	140	62 Rc

ROLLING-CONTACT SLIP CHARACTERISTICS

The crystal structure of MgO is of the NaCl type, which is characterized by two interpenetrating face-centered cubic (fcc) lattices of the oppositely charged ions. The number of available slip planes is normally limited to the six {110} cube-diagonal planes. This is because the MgO bonding is strongly ionic and high energy barriers resulting from like-charged ions being placed in close proximity prevent slip on the more closely packed {100} cube planes. Normally, the most closely packed planes in solids are the

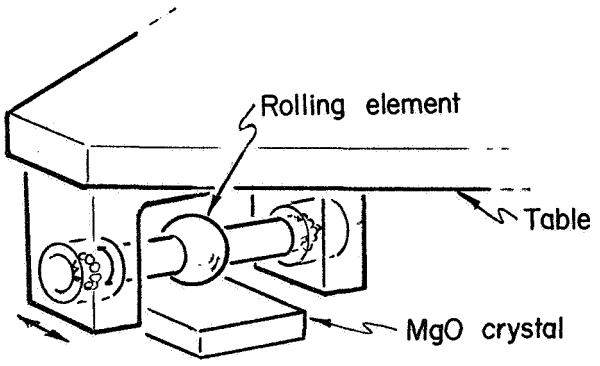

a. Reciprocating Rolling

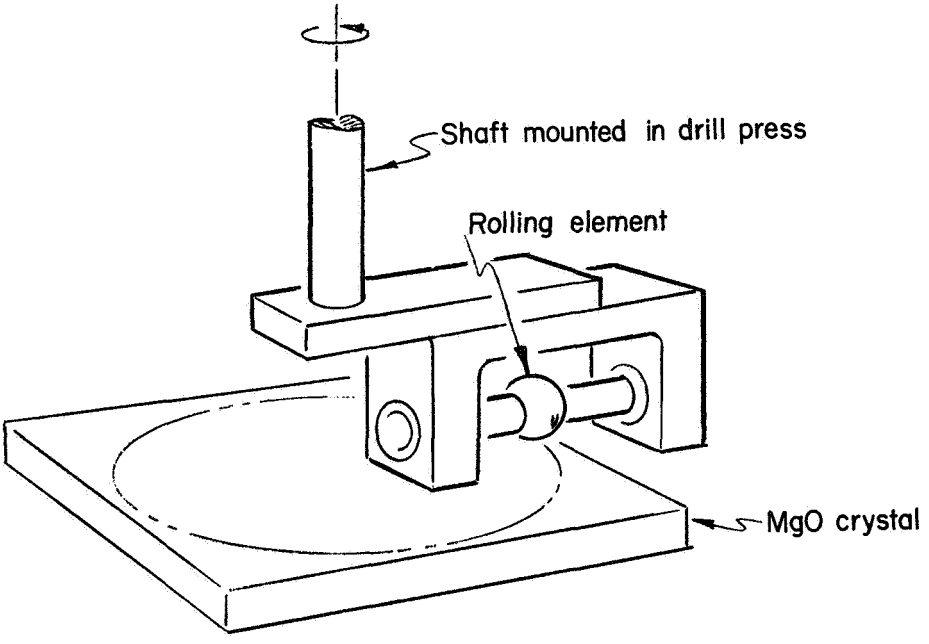

b. Elastohydrodynamic Rolling

FIGURE 1. CONFIGURATION FOR APPLYING ROLLING-CONTACT STRESS

active slip planes. These limited and relatively simple slip characteristics of MgO make the interpretation of slip resulting from the localized and complex rolling-contact stresses more straightforward than would be possible in solids with more complicated slip characteristics.

The active slip planes and crystallographic directions are shown in Figure 2. The {110} slip planes that intersect the surface at 45 degrees (2a) are referred to as $\{110\}_{45}$ slip planes, and those intersecting the surface at 90 degrees (2b) are referred to as $\{110\}_{90}$ slip planes. Dislocations on the slip planes are depicted as loops that intersect the surface at their two ends. The $\{110\}_{45}$ slip planes contain loops that intersect the (001) cleavage plane as screw dislocations (denoted by "S" in Figure 2a). The $\{110\}_{90}$s intersect in the edge configuration (Figure 2b). The point of intersection with the surface can be detected in MgO by etching with a solution of 10 percent saturated NH_4Cl and 30 percent HCl for 20 minutes. The resulting etch pits tend to line up to show the straight-line intersection of the slip plane and surface. The preferred slip planes that operate with a rolling-contact stress are shown in Figure 3. The etch-pit patterns expected on a cleaved cross section normal to the ball path are also shown.

The actual etch-pit patterns on a typical surface and cross section are shown in Figure 4. Rows of dislocation etch pits lie both parallel and normal to the [100] ball rolling direction, which result from slip on the $\{110\}_{45}$ planes seen in Figures 2 and 3. In the cross section, the $\{110\}_{45}$ planes that intersect the surface parallel to the rolling direction cross beneath the surface. The crossing point has been shown to be very near the calculated maximum Hertzian shear stress and is probably where the dislocations are generated.[1] Also seen in the cross section is the deeper penetration of the $\{110\}_{45}$ slip planes that are parallel to the rolling direction and are inclined at 45 degrees to the surface on the cross section. This results from the stress field moving parallel to these planes and therefore influencing the dislocations for a greater time than those lying on the $\{110\}_{45}$ slip planes that intersect the surface normal to the rolling direction.

While numerous other observations in previous work have been reported, the basic slip characteristics described above will permit an understanding of the experimental results that are the subject of this report.

EXPERIMENTAL RESULTS AND DISCUSSION

Reciprocating Rolling

The following results are an extension of the experiments performed under Task Order No. 4 of Contract NAS 3-6263.

Track Hardness

Previous measurements of the variation of track width with rolling cycles on MgO showed an initial width increase, a plateau, and, finally, a second increase after 10^4 cycles.[2] Spalling often was observed during the second width increase. Although the

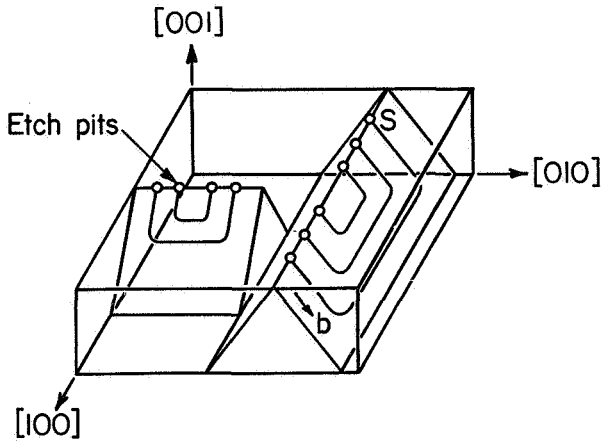

a. $\{110\}_{45°}$ Slip Planes

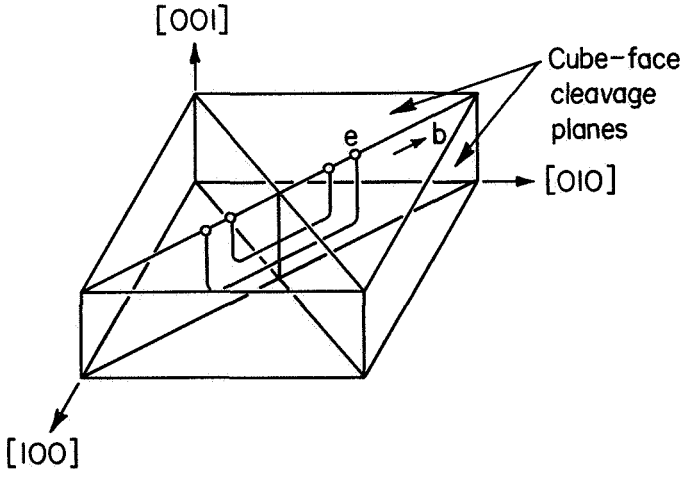

b. $\{110\}_{90°}$ Slip Planes

FIGURE 2. CRYSTALLOGRAPHIC DIRECTION AND SLIP PLANES IN MAGNESIUM OXIDE

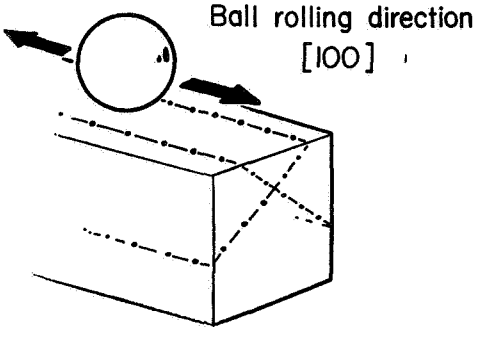

a. (101) and ($\bar{1}$01) Slip Planes

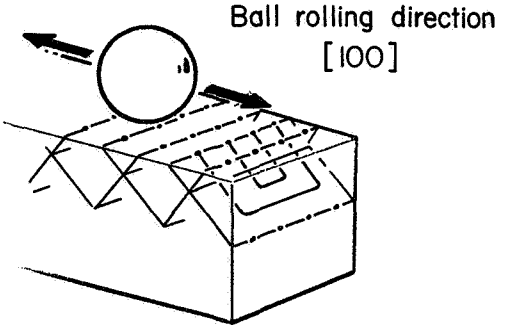

b. (011) and (0$\bar{1}$1) Slip Planes

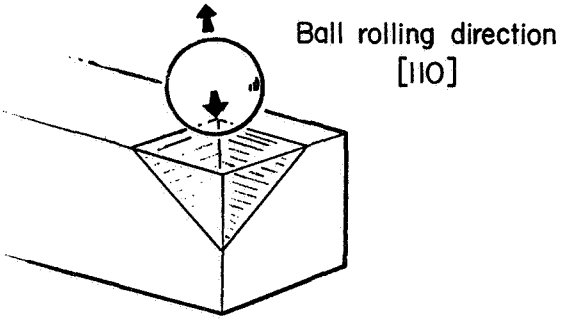

c. (101) and (011) Planes Intersecting at 120° in Front of Ball Rolling in [110] Direction

FIGURE 3. PREFERRED SLIP SYSTEMS IN SINGLE-CRYSTAL MgO FOR VARIOUS BALL ROLLING DIRECTIONS

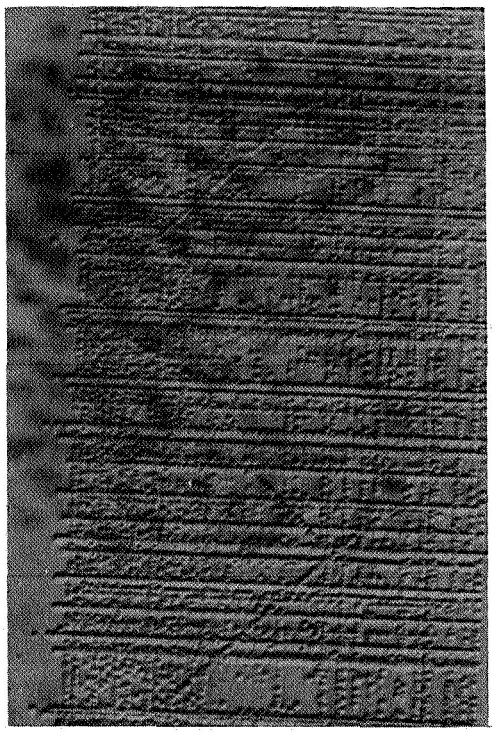

[100] Rolling Direction

500X

a. Surface

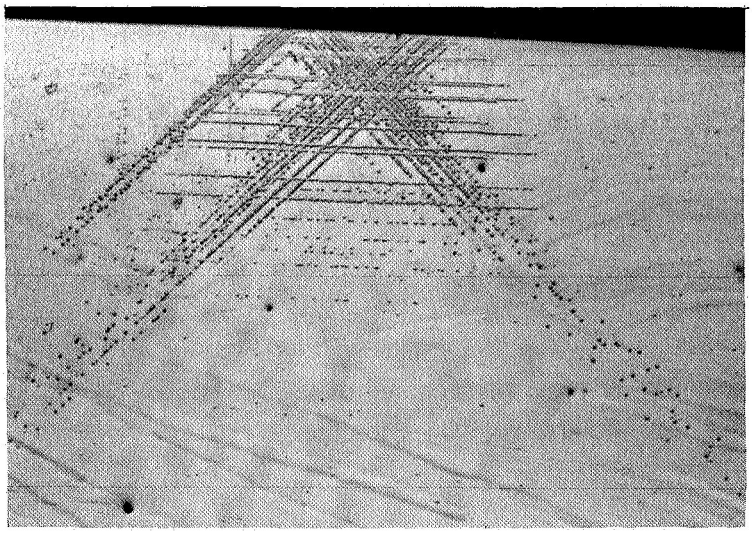

200X

b. Cross Section

FIGURE 4. DISLOCATION ETCH-PIT PATTERNS AFTER ONE ROLLING-CONTACT PASS AT A 570-GRAM LOAD

track width was assumed to be a measure of plastic deformation of the track since measurements of ball and track wear could not explain the width increases, a more direct measure of plastic deformation was desired. Microhardness, which is influenced by dislocation density and interaction resulting from plastic deformation, was evaluated as a possible technique.

Rolling-contact tracks were made in both the [100] and [110] directions with 244-g (0.54 lb) and 570-g (1.26 lb) load under dry rolling conditions. Tracks were made on the same specimen with 1, 10, 10^2, 10^3, 10^4, 10^5, and 10^6 rolling-contact cycles. Ten Knopp-hardness measurements were made in each track to measure the microhardness. A 100-g (0.22 lb) indenter load was used, and the long axis of the diamond was oriented in the [100] direction. Hardness measurements made with the long axis in the [100] direction showed the material to be softer and to tend toward cleavage failure under the impression, which demonstrates the anisotropy of MgO.

The results of the microhardness tests are shown in Figures 5 and 6. Each point is an average of the 10 microhardness readings. A considerable difference in hardness was recorded among the undeformed crystals, which reflects a difference in original mechanical properties. This result identified the necessity of using specimens from the same bulk crystal to reproduce experimental results for comparison purposes.

Both the [100] and [110] rolling directions showed a significant hardness increase after only one rolling-contact cycle. Even though the dislocation density was low and readily resolvable by etch-pit techniques after one cycle, sufficient dislocation interaction had occurred to cause the hardness increase. The dislocation interaction during the first few cycles of stress was revealed in electron microscope studies discussed later. A further hardness increase was measured after 10 rolling-contact cycles for both rolling directions. A plateau was then observed similar to the plateau in the track-width measurements. However, the plateau was smaller for tracks made with a 570-g (1.26 lb) ball load, since the hardness began to increase again after 10^3 cycles whereas the track width did not begin a second increase until 10^4 cycles. Hardness and track width behaved similarly for tracks made with a 244-g (0.54 lb) load throughout the entire cycle range.

Although the Knoop microhardness measurements are subject to uncertainty at such high hardness levels and are influenced strongly by local property variations of the track, a significant trend in hardness with rolling cycles was measured. The general shape of the microhardness curves is similar to the previous track-width curves. The track-width increases are therefore associated with track hardness increases. Hardness increases in MgO could conceivably result from several causes, which include precipitation of second-phase impurity particles, creation of point defects, pinning of dislocations by impurity atoms, creation of subgrain boundaries, and increases in dislocation density and interaction. Since increases in dislocation density and interaction would be the predominant hardening mechanism, they are probably responsible for the increases in track width and hardness. The increases continue to 10^6 cycles, where track spalling occurs.

Thin-Film Electron Microscopy

Although track-width and hardness measurements give an indication of plastic deformation of the rolling-contact track on MgO, a direct observation of dislocation

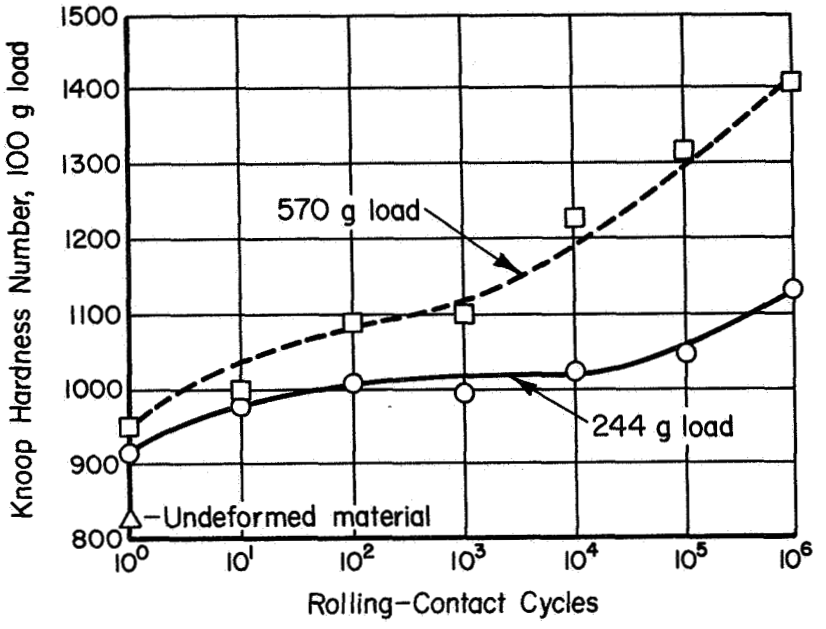

FIGURE 5. VARIATION OF TRACK HARDNESS WITH ROLLING-CONTACT CYCLES UNDER DRY CONDITIONS IN [100] ROLLING DIRECTION

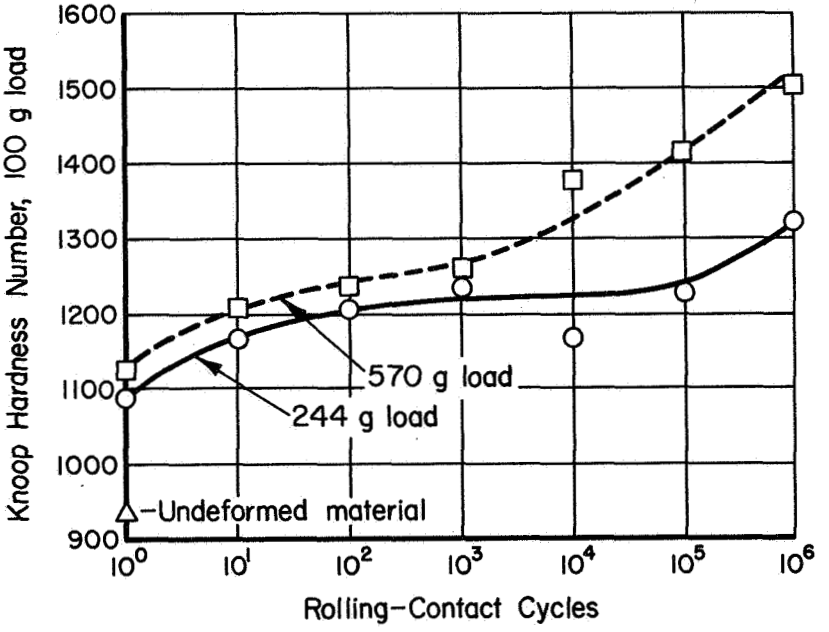

FIGURE 6. VARIATION OF TRACK HARDNESS WITH ROLLING-CONTACT CYCLES UNDER DRY CONDITIONS IN [110] ROLLING DIRECTION

interactions that may be responsible for fatigue spalling is required to understand the progressive damage resulting from repeated application of rolling-contact stress cycles. Polarized light and X-ray topography are both very sensitive to lattice strains resulting from plastic deformation in MgO, but attempts to study dislocations in rolling-contact tracks proved that neither had the required resolving power. Thin-film transmission electron microscopy was therefore necessary to resolve dislocations occurring in high concentrations after repeated rolling-contact stress cycles.

Previous observation of thin films of MgO by transmission electron microscopy revealed that dislocations apparently moved away from the thinnest regions during the thinning process. The thicker areas surrounding the thin regions retained the original dislocation configurations, but the dislocations were difficult to resolve because of increased section thickness. The thick sections cause electron-beam scattering and transmitted intensity decreases that limit observations to lower magnifications. A diffusion-locking technique was used to circumvent this problem. A low-temperature anneal was given the specimens prior to thinning to diffuse an "atmosphere" of foreign atoms to the dislocation lines. The energy associated with the dislocation is lowered, which greatly hinders further movement.

Preparation of specimens for viewing in the electron microscope began with a series of closely spaced rolling-contact tracks on the surface with the desired number of cycles. Specimens were made with tracks of 10, 10^2, 10^3, and 10^5 rolling-contact cycles. The bulk specimens were given a 3-hour, 600 C anneal and furnace cooled to permit diffusion of impurity atoms to the dislocation lines. MgO crystals normally contain approximately 0.2 percent impurity atoms, which is a sufficient quantity for effective locking. The bulk crystal was cleaved into specimens of suitable size for the stage in the electron microscope. The top surface and sides of the specimen were coated with an acid-resisting plastic to permit thinning from the back surface without removing the track region. A hot jet of orthophosphoric acid was used to thin the specimens to approximately 10 microns (390 microinches) at the center. The acid-resisting plastic was maintained on the surface during this portion of the thinning to ensure a thin film in the track region. Further thinning until interference fringes were observed under a light microscope was done in a dish of hot orthophosphoric acid with the acid-resisting plastic removed. A 2:1 solution of orthophosphoric acid and ethyl alcohol at room temperature was used to slow the thinning rate for further thinning until first-order interference fringes were observed. The specimens were finally coated with an evaporated film of carbon to make them electrically conducting for viewing in the electron microscope.

Representative areas from four tracks with increasing rolling-contact cycle levels are shown in Figures 7, 8, 9, and 10. Undeformed MgO had a very low concentration of random grown-in dislocations. Extensive dislocation interactions were visible after only 10 rolling-contact cycles as shown in Figure 7. It was evident that, even at an early stage in the deformation process, the dislocation configurations resulting from rolling-contact stress were not simple straight loops. The field consisted essentially of some jogged lines but mostly dipoles. Considerable dislocation interaction was evidenced from these configurations. Dislocation density and interaction increased slightly between 10 and 10^2 rolling-contact cycles, as shown in Figure 8. There is indication of concentration and tangling of dipoles. Little change in dislocation density and interaction was observed between 10^2 and 10^3 rolling-contact cycles, see Figure 9. This initial initial increase in dislocation density and interaction, followed by a relatively unchanged configuration to 10^3 rolling-contact cycles, can be directly related to the similar behavior of the track-width and hardness measurements. Presumably, dipole drag and

35,000X J16662

FIGURE 7. DISLOCATION CONFIGURATION AFTER 10 ROLLING-CONTACT CYCLES WITH 570-G (1.26 LB) LOAD

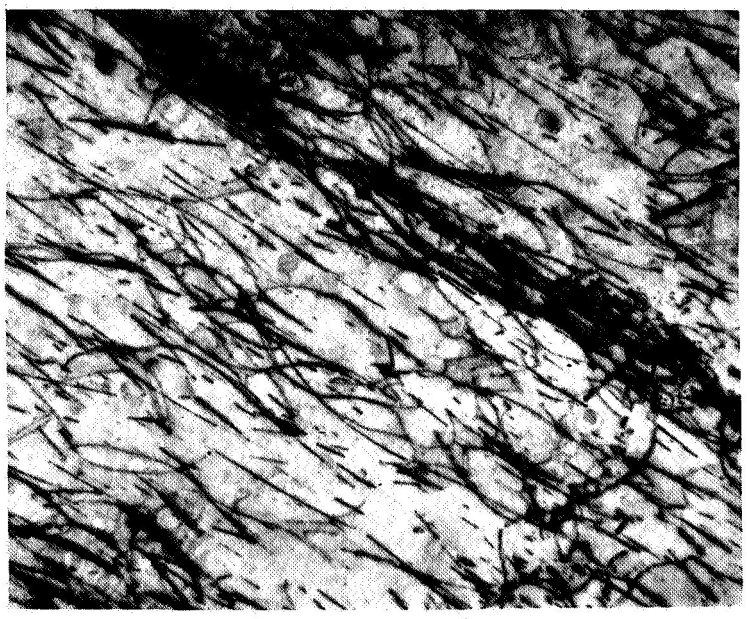

35,000X J16665

FIGURE 8. DISLOCATION CONFIGURATION AFTER 10^2 ROLLING-CONTACT CYCLES WITH 570-G (1.26 LB) LOAD

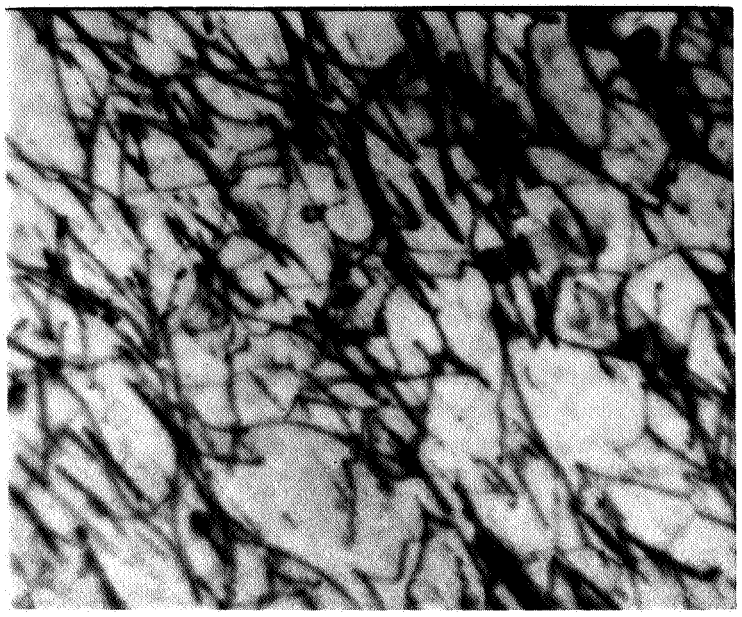

35,000X J16673

FIGURE 9. DISLOCATION CONFIGURATION AFTER 10^3 ROLLING-CONTACT CYCLES WITH 570-G (1.26 LB) LOAD

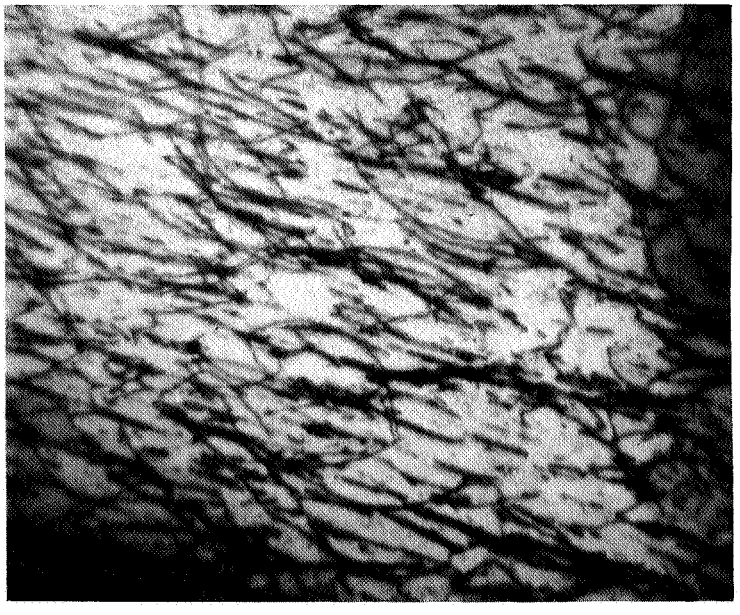

35,000X J16749

FIGURE 10. DISLOCATION CONFIGURATION AFTER 10^5 ROLLING-CONTACT CYCLES WITH 570-G (1.26 LB) LOAD

tangling produced a hardening effect. The results of the thin-film examination therefore confirm that track-width and hardness measurements directly reflect dislocation density and interaction. The dislocation configuration after 10^5 rolling-contact cycles, Figure 10, showed an increase in dislocation density and a reduction in the size of dipoles when compared with Figure 9 (10^3 rolling-contact cycles). There is also an indication of increase in the density of dislocation tangles. The second increase in track width and hardness therefore also reflected a change in dislocation configuration. These results clearly indicate that changes in the properties of the track during application of rolling-contact stress result from changes in the dislocation configuration even at high levels of rolling-contact cycles.

No dislocation interactions associated with crack nucleation were observed in the thin films examined. Since crack locations occur randomly along the tracks, examination of thin films from numerous tracks would probably be required to insure observation of an embryo fatigue crack. Concentration of dislocation segments and dipoles into intersecting ribbons may be the resulting structure after a large number of rolling-contact cycles that produce embryo cracks at intersections.

Depth of Dislocation Penetration

Measurements of depth of dislocation penetration, or slip depth, in Task Order No. 4 showed a decrease with increasing ball rolling velocities.[2] The relationship between the dislocation velocity, applied stress, and time of application of the stress qualitatively predicted the decrease. Experiments were performed under the present Task Order No. 5 to determine whether the decrease in slip depth at high rolling velocities persisted with repeated stress cycles.

All specimens were cleaved from the same bulk crystal to permit comparison of results. Tracks were made in the [100] rolling direction with a 570-g (1.26 lb) ball load at rolling velocities of 1.59×10^{-2} cm/sec (6.26×10^{-3} in./sec), 9.53×10^{-1} cm/sec (3.75×10^{-1} in./sec), and 2.75 cm/sec (1.08 in./sec). The specimens were cleaved four times normal to the track in the central one-third region. The depth of slip was measured with a filar eyepiece from the surface to the end of the slip lines formed by the $\{110\}_{45}$ planes that lie parallel to the rolling direction. Ten readings were averaged for each condition.

The relationship between depth of slip and rolling-contact cycles for the three rolling velocities is shown by graph in Figure 11. The slip depth is strongly dependent on rolling velocity, which becomes more pronounced at higher levels of rolling-contact cycles. Higher rolling velocities tend to reduce the first slip-depth increase after one cycle as well as the increase after 10^4 cycles. Measurements were not obtained at 10^4, 10^5, and 10^6 cycles for the lowest rolling velocity because of the extended times required to obtain the high-cycle levels.

The dependency of depth of slip on rolling velocity at high cycle levels suggests a more complicated relationship than a simple lack of time for dislocation propagation at high rolling velocities. If sufficient time were the only requirement, the high number of stress applications should allow the dislocations propagating from tracks of high rolling velocity to eventually reach depths equal to those produced with low rolling velocities. More extensive dislocation interaction near the surface of high-rolling-velocity tracks may be responsible. With dislocation movement restricted to shallower depths at low

cycle levels, effective dislocation pinning and locking may be occurring which will hinder further penetration into the crystal.

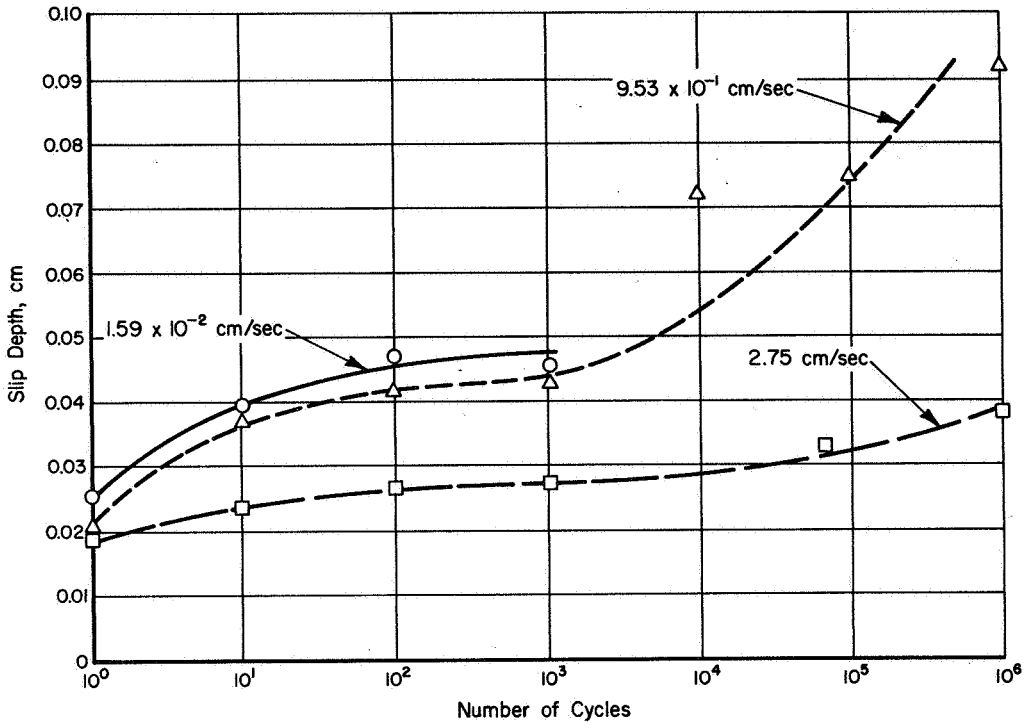

FIGURE 11. VARIATION OF SLIP DEPTH WITH ROLLING-CONTACT CYCLES AT THREE ROLLING VELOCITIES

The general shape of the slip-depth curves is similar to the track-width and hardness curves. An initial increase is seen, followed by a plateau and a second increase. While dislocation interactions are the most likely cause of fatigue-crack formation in MgO, increased depth of dislocation penetration is also associated with the cycle range that spalling occurs.

Adsorbed Fluids

Studies in Task Order No. 4 revealed a marked change in slip mode caused by the presence of lubricants on MgO surfaces subjected to rolling-contact stresses.[2] Slip on $\{110\}_{90}$ planes became predominant, and spalling occurred within 10^3 rolling-contact cycles. Although a surface interaction with the lubricants causing a change in dislocation mobility was suspected, the cause of the unexpected effect of lubricants was not determined.

The influence of adsorbed fluids on plastic flow properties has been under investigation since P. A. Rebinder's discoveries in 1928. More recent studies[3,4,5] on the effect of adsorbed liquids on the microhardness of oxides, alkali halides, and semiconductors have shown that the presence of adsorbed liquids can greatly influence dislocation mobility of these materials near the surface. The presence of water, organic molecules of different dipole moments, and ions in aqueous solutions were capable of

causing hardness changes through influencing dislocation mobility. Since the rolling-contact state of stress is somewhat analogous to that of microhardness impressions, a similar effect on dislocation mobility was expected.

The liquids dimethyl formamide (DMF), water, and toluene were selected for study because of their different dipole moments*: 3.8, 1.8, and 0.4 Debye units**, respectively. In addition to the difference in dipole moments, toluene prevents adsorption of water on the surface and DMF preferentially adsorbs from an aqueous solution. Comparison of the effects of the three liquids on the same specimen was therefore possible.

Specimens were prepared by the normal cleaving and acid-polishing techniques. The adsorbed water was removed from the surfaces by baking at 300 C under dynamic vacuum, and the specimens were encapsulated under vacuum to prevent readsorption of water. The capsules were broken open under fresh toluene obtained from a new sealed bottle. Toluene has a low, but not negligible, solubility for water, which prevents adsorption of water on the MgO surface for at least an hour. The rolling-contact experiments were immediately conducted with the specimen and the ball flooded with toluene. Tracks with 10^2 and 10^3 rolling-contact cycles were made in the [100] rolling direction with a 560-g (1.26 lb) ball load. The specimen was removed from the toluene and swabbed with cotton under warm water for 15 minutes. A similar pair of tracks with 10^2 and 10^3 rolling-contact cycles were made under water next to the tracks made under toluene. The specimen was then swabbed under DMF for 1 hour, and a third pair of tracks with 10^2 and 10^3 rolling-contact cycles were made under DMF. This procedure permitted a direct comparison of the effect of the three liquids on the same specimen.

A marked difference was observed in the rolling-contact tracks made under toluene compared with water and DMF. Figure 12 shows a typical area after 10^3 rolling-contact cycles under toluene. Extensive slip on $\{110\}_{90}$ planes, track spalling, and subsurface cleavage (circular light areas in Figure 12) were apparent after 10^3 rolling-contact cycles. This behavior was identical to that observed in Task Order No. 4 with oil on the surface.[2] Typical areas after 10^3 rolling-contact cycles under water and DMF are shown in Figures 13 and 14. The track made under water was identical to those observed in "dry" experiments performed in normal laboratory air. Enough water vapor is probably available to the surface in air to produce essentially the same adsorbed surface layer as immersion in water. The tracks made under DMF, Figure 14, were similar to the track made under water, but had some $\{110\}_{90}$ slip plane "wings" similar to those occasionally observed in "dry" experiments.

The track widths were nearly identical after 10^2 cycles with all three liquids. After 10^3 cycles, the DMF track width remained unchanged from 10^2 cycles; the water track width increased by 27 percent; and the toluene track width increased by 67 percent. Toluene, the lowest dipole-moment liquid tested, therefore caused $\{110\}_{90}$ slip, track widening, and early spalling. No spalls were observed on the DMF and water tracks, but track width appeared to be influenced by the particular fluid present. The highest dipole-moment liquid, DMF, inhibited track widening, while water had an intermediate effect. The similarity in rolling-contact tracks made under oil and toluene suggest that the same mechanism is responsible. Since toluene has a very low viscosity and the

*The dipole moment of a polar molecule is a vector quantity equal to the product of the electronic charge and the relative displacement of the positive and negative electrical centers. It is a measure of the polarity of the molecule.
**10^{-18} electrostatic-cm units.

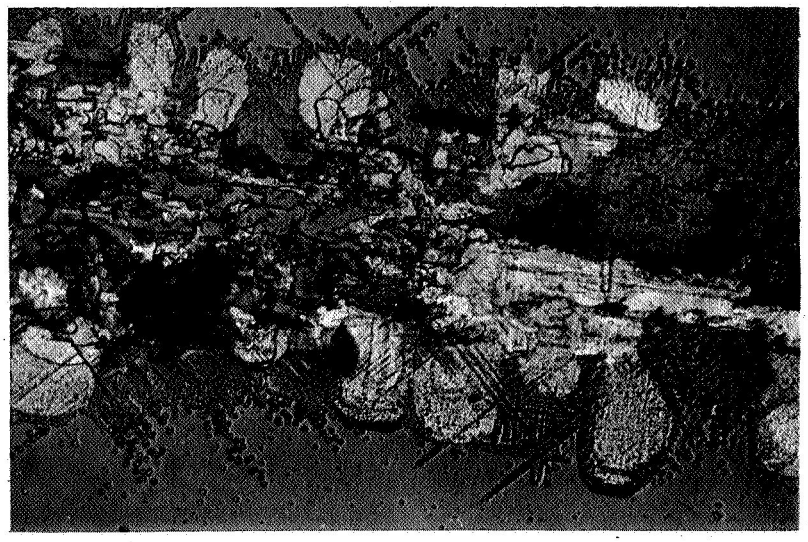

200X

FIGURE 12. TRACK AFTER 10^3 ROLLING-CONTACT CYCLES UNDER TOLUENE, [100] ROLLING DIRECTION, 570-G (1.26 LB) LOAD

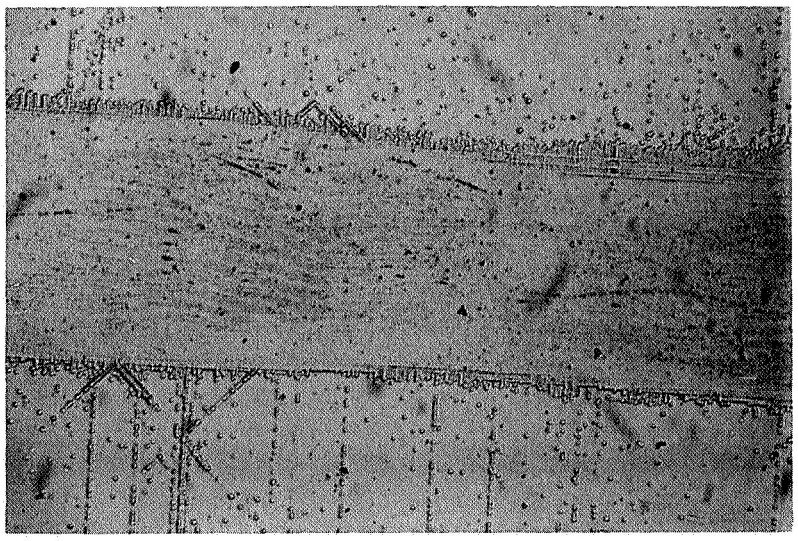

200X

FIGURE 13. TRACK AFTER 10^3 ROLLING-CONTACT CYCLES UNDER WATER, [100] ROLLING DIRECTION, 570-G (1.26 LB) LOAD

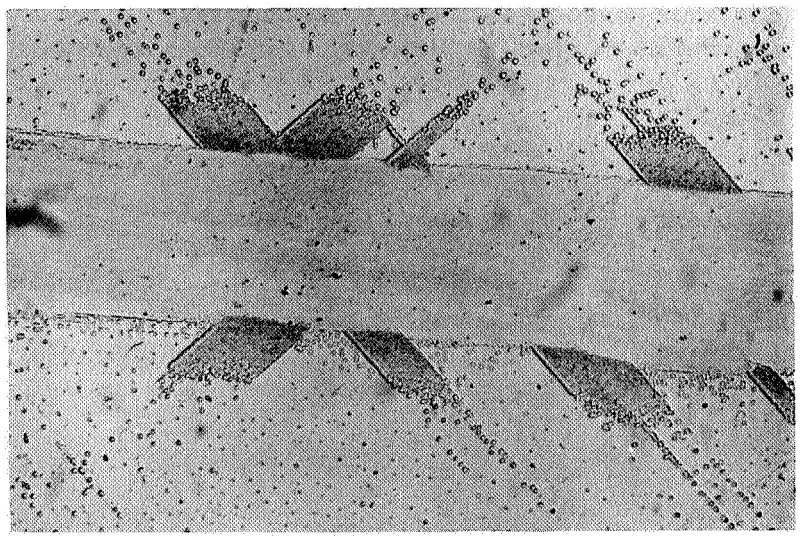

FIGURE 14. TRACK AFTER 10^3 ROLLING-CONTACT CYCLES UNDER DMF, [100] ROLLING DIRECTION, 570-G (1.26 LB) LOAD

rolling speeds were low, a change in contact pressure resulting from elastohydrodynamic films was probably not responsible. The influence of the adsorbed liquids on dislocation mobility appears to be the most likely cause.

The results of hardness studies have shown that edge-dislocation mobility increases and hardness decreases with increasing dipole moment of the adsorbed liquid.[4,5] The mobility of edge dislocations (active on $\{110\}_{90}$ slip planes, which intersect the [100] track at 45 degrees) increases in this order: toluene, water, and DMF. The influence on screw dislocation mobility was not reported. The influence of these liquids on track width in MgO was in the opposite order; toluene, which decreases dislocation mobility, produced the widest tracks. This effect may have resulted from the track having a greater resistance to conforming plastically to the ball as a result of the decreased dislocation mobility and increased hardness. The track would remain flatter, and the maximum Hertzian shear stress would be higher and would occur deeper in the MgO. Dislocations initiating at the point of maximum Hertzian stress on $\{110\}_{45}$ planes would reach the surface farther from the centerline of contact, which would result in a wider track. Track-depth measurements made with an interference microscope confirmed this hypothesis. The water and toluene tracks (in an unspalled region) were approximately 12 microinches (0.31 microns) deep, while the DMF track was 20 microinches (0.51 microns) deep. The narrowest track was also the deepest, which indicates the MgO had plastically conformed to the ball. Therefore, track width does not necessarily reflect the extent of plastic deformation.

While the alteration in dislocation mobility by adsorbed liquids can explain the change in track width, the reason for extensive slip on $\{110\}_{90}$ planes with toluene (and oil) on the surface is not readily explained by this concept. This effect could result if the mobility of screw dislocations was decreased more than edge dislocations. Dislocations meeting the surface on $\{110\}_{45}$ planes are screw dislocations. Since the mobility of edge dislocations is normally much greater than screw dislocations in MgO, decreases in screw dislocation mobility by adsorbed liquids could be effectively pinning them. Slip would then occur by edge dislocations, or on the $\{110\}_{90}$ planes.

In further hardness studies on the influence of adsorbed liquids on dislocation mobility, various concentrations of AgCl and dimethylsulfoxide (DMSO) in aqueous solutions have affected the hardness and dislocation mobility in MgO in a complex manner.[6] Rolling-contact experiments with the concentrations reported to raise and lower dislocation mobility from that of pure water showed no change in track width or slip characteristics. Apparently, the dislocation mobility under rolling-contact conditions was not affected as greatly as with toluene and DMF.

The studies of dislocation mobility by hardness measurements have shown the influence of adsorbed liquids to be quite complicated. Originally, this Rebinder effect was thought to be caused by selective adsorption at dislocation sites and subsequent "adsorption locking" of dislocations that terminate at the surface. However, the electronic structure of the adsorbed species, the energy-band configuration near the surface, and the influence of impurities on the electron or hole-transfer processes now appear to be important.[4] How these conditions affect the rolling-contact characteristics on MgO remains to be determined.

Elastohydrodynamic Rolling

Since actual rolling-contact bearings usually operate at rolling velocities high enough to generate elastohydrodynamic oil films that separate the rolling elements, the effect of such films on the basic deformation processes are of interest. The sensitivity of dislocation motion in MgO to modifications in applied stress make it a useful material for these studies, also.

Film-Thickness Calculations

The thickness of elastohydrodynamic oil films expected between the 0.25-inch (0.64 cm)-radius steel balls and the MgO flats was calculated using Grubin's theory[7] and modifications of Grubin's theory resulting from experimental studies by Kannel[8] to establish the required operating conditions to produce elastohydrodynamic films. The following constants were used in the calculations:

	MgO	AISI 52100 Steel
Young's Modulus	38×10^6 psi (2.7×10^4 kg/mm^2)	30×10^6 psi (2.1×10^4 kg/mm^2)
Poisson's Ratio	0.25	0.30

Lubricant viscosity at 72 F = 340 cp.
Ball load = 0.54 lb (244 g).

With these constants, the following values of film thickness were calculated:

Rolling Velocity		Elastohydrodynamic Film Thickness			
		Grubin's Theory		Kannel Modification	
In./Sec	Cm/Sec	Microinches	Microns	Microinches	Microns
2.1	5.3	0.6	0.015	0.2	0.005
5.9	15	1.3	0.033	0.5	0.013
15	38	2.6	0.066	0.9	0.024
24	61	3.7	0.094	1.2	0.031
30	76	4.4	0.11	1.4	0.036
60	152	7.2	0.18	2.3	0.058
120	305	11.9	0.30	3.6	0.092
240	610	19.8	0.50	5.8	0.15

Since rolling velocities of at least 60 in./sec (152 cm/sec) were required to produce film thicknesses comparable to the surface finish of the ball, the reciprocating motion used in all previous experiments was not applicable. Unidirectional rolling in circular paths on MgO flats was therefore adopted. The standard 0.25-inch(0.635 cm)-diameter shaft-mounted steel ball was mounted eccentrically in a 5200-rpm drill press to impart circular motion. The eccentricity was adjustable to permit up to six circular tracks of different diameters on the 3/4 x 3/4-inch (1.9 x 1.9 cm) MgO flats. The resulting rolling velocities were between 96 and 188 in./sec (244 and 478 cm/sec). A 244-g (0.54 lb) ball load was used in all experiments. Rolling was performed dry, with 350 cs, DC 200 silicone oil, or with OS124 polyphenyl ether. Electrical continuity measurements with a steel plate substituted for the MgO flat confirmed that an elastohydrodynamic oil film was being generated during rolling with the two oils.

Track Characteristics

The dislocation slip mode in tracks made under elastohydrodynamic rolling conditions was distinctly different from the low-speed-reciprocating-rolling tracks. Figure 15 shows a typical track area after 85 rolling-contact cycles. Slip occurred in concentrated bands on $\{110\}_{45}$ planes, rather than uniformly across the track as occurred in reciprocating-rolling experiments. Measurements with an interference microscope showed that the bands were grooves approximately 16 microinches (0.41 microns) below the undeformed MgO surface. The undeformed areas in the track between the bands were 8 microinches (0.2 microns) below the undeformed surface, or 8 microinches (0.2 microns) above the bands. As the number of cycles increased, the bands gradually widened. Figure 16 shows a typical area after 260 cycles. After 10,000 cycles, the bands had nearly converged (Figure 17), which made the track appear similar to the low-speed-reciprocating-rolling tracks. The bands were also visible on cleaved cross sections of the track. Figure 18 shows the subsurface dislocation configuration after 520 rolling-contact cycles. Bands resulting from slip on both systems of $\{110\}_{45}$ slip planes are visible. No evidence of extensive slip on $\{110\}_{90}$ planes was seen, unlike the low-speed-reciprocating-rolling experiments with oil and toluene. No differences in slip characteristics were observed when OS 124 polyphenyl ether was used in place of DC 200 silicone oil.

Experiments using the high rolling velocities without oil showed that extensive track and ball damage occurred rapidly. After only 260 cycles, the track had many small pitted areas such as seen in Figure 19. Activation of the $\{110\}_{90}$ slip planes was also apparent. The pitting became more extensive as the number of cycles increased, and before 5000 cycles the entire track region was spalled away. Once several spalls were formed in the track, the damage propagated rapidly from the resulting vibration and pounding. Because of the severe ball and track damage, experiments with high-speed dry rolling were not persued.

Track-Width and Hardness Measurements

Track widths and hardnesses were measured on a series of tracks on MgO made under elastohydrodynamic rolling conditions. OS 124 polyphenyl ether was the lubricant. Concentric tracks with 10^2, 10^3, 10^4, 10^5, and 10^6 cycles were made on each specimen to permit direct comparison. Hardness measurements were taken from Knoop impressions made with a 100-g (0.22 lb) load. Hardness measurements were not made on tracks with fewer than 10^4 cycles because of the restriction of deformation to narrow bands at the low-cycle levels. Tracks with fewer than 100 cycles were not obtained because of the very short running times required.

The hardness and track-width measurements are plotted in Figure 20. The shapes of the curves are different from those obtained with reciprocating, slow speed, dry rolling. The track width under elastohydrodynamic rolling conditions increased rapidly between 10^2 and 10^4 cycles and remained unchanged between 10^4 and 10^6 cycles. The hardness increased between 10^4 and 10^5 cycles and remained constant between 10^5 and 10^6 cycles. In the previous experiments, the track width and hardness increased to an equilibrium value in less than 10^2 cycles, remained constant between 10^2 and 10^4 cycles, and then increased again between 10^4 and 10^6 cycles. A typical track-width curve is plotted in Figure 20 for comparison. The maximum track width after 10^6 cycles of

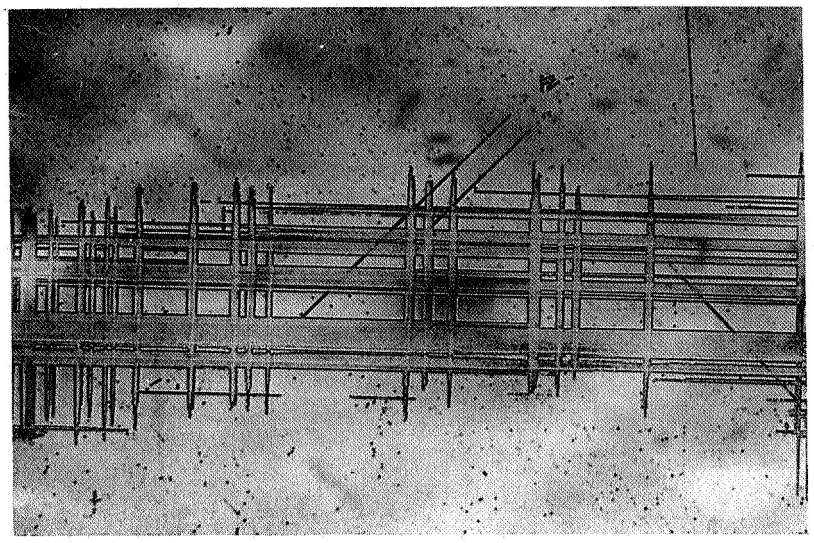

100X

FIGURE 15. DISLOCATION CONFIGURATION AFTER 85 CYCLES OF ELASTOHYDRODYNAMIC ROLLING

244-g (0.54 lb) load, 350 cs DC 200 silicone oil, 150-in./sec (380 cm/sec) rolling velocity, [100] rolling direction.

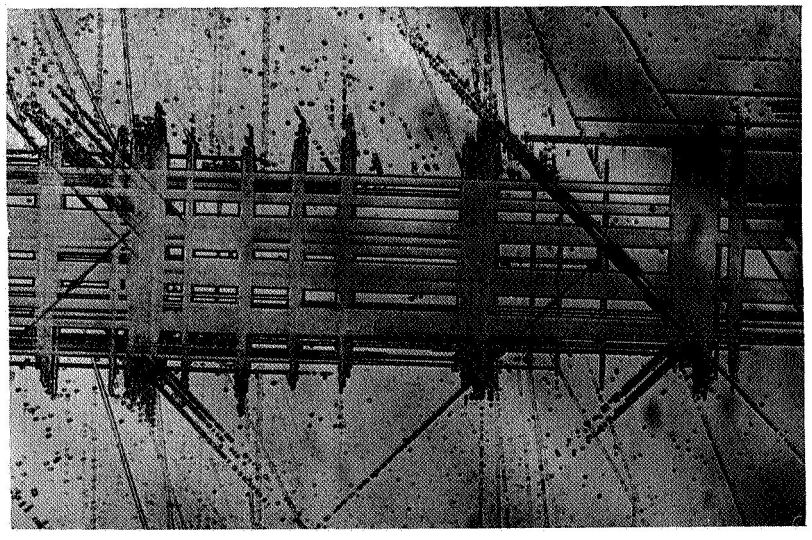

100X

FIGURE 16. DISLOCATION CONFIGURATION AFTER 260 CYCLES OF ELASTOHYDRODYNAMIC ROLLING

244-g (0.54 lb) load, 350 cs DC 200 silicone oil, 150-in./sec (380 cm/sec) rolling velocity, [100] rolling direction.

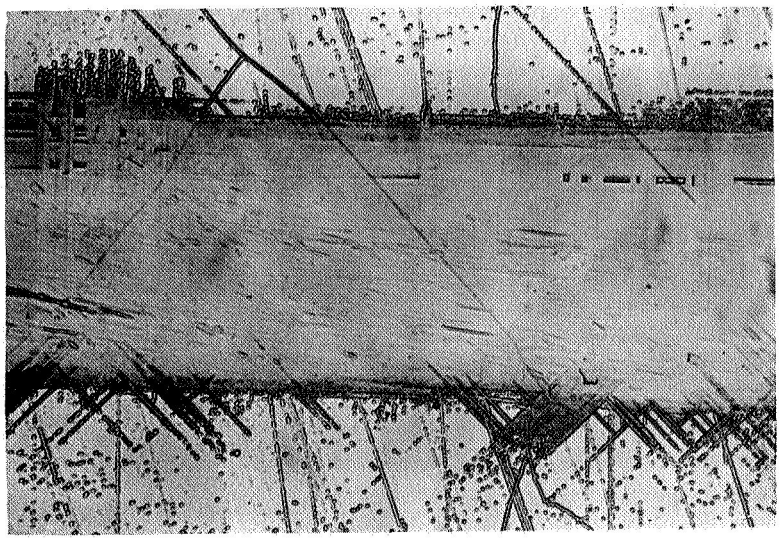

100X

FIGURE 17. DISLOCATION CONFIGURATION AFTER 10,400 CYCLES OF ELASTOHYDRODYNAMIC ROLLING

244-g (0.54 lb) load, 350 cs DC 200 silicone oil, 190-in./sec (480 cm/sec) rolling velocity, [100] rolling direction.

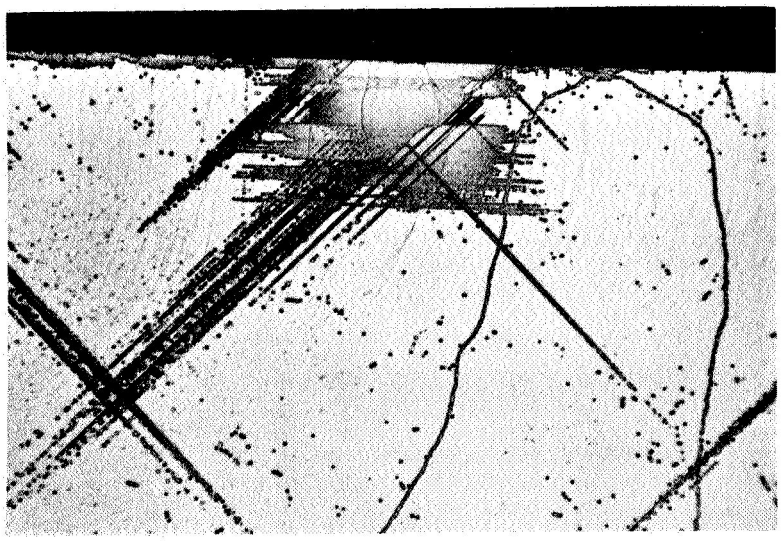

100X

FIGURE 18. DISLOCATION CONFIGURATION ON CROSS SECTION OF TRACK AFTER 520 CYCLES OF ELASTOHYDRODYNAMIC ROLLING

244-g (0.54 lb) load, 350 cs DC 200 silicone oil, 167-in./sec (425 cm/sec) rolling velocity, [100] rolling direction.

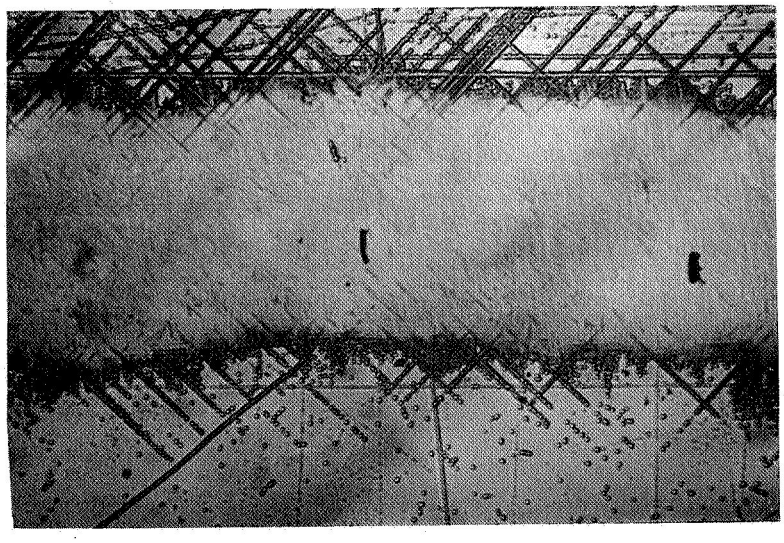

100X

FIGURE 19. DISLOCATION CONFIGURATION AFTER 260 CYCLES OF DRY ROLLING

244-g (0.54 lb) load, 96 in./sec (240 cm/sec) rolling velocity, [100] rolling direction.

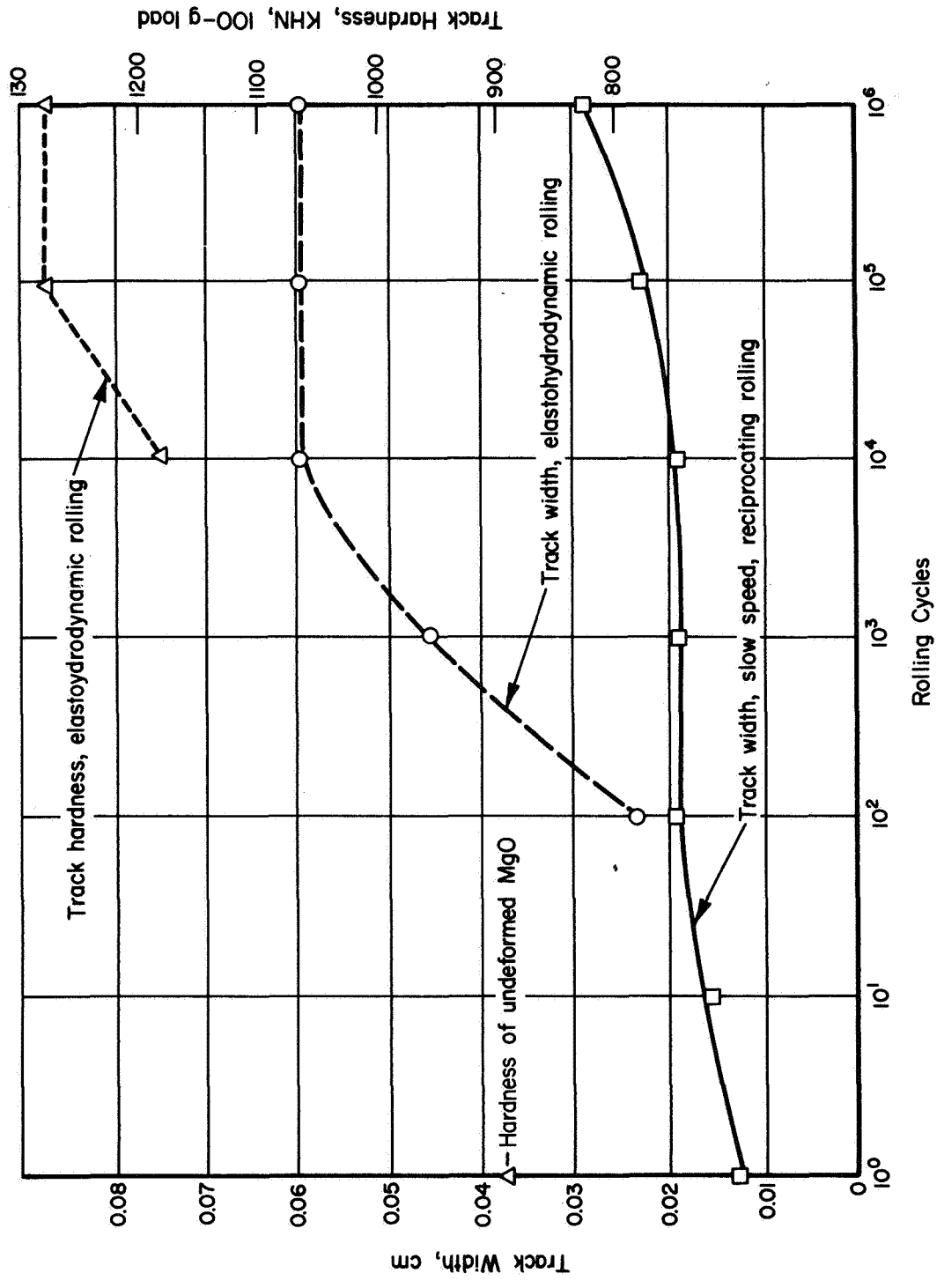

FIGURE 20. VARIATION OF TRACK WIDTH AND HARDNESS ON MgO WITH ROLLING CYCLES UNDER ELASTOHYDRODYNAMIC CONDITIONS. 244-g BALL LOAD, 364 cm/sec (143 in./sec) AVERAGE ROLLING VELOCITY. TRACK WIDTH FOR SLOW SPEED, RECIPROCATING ROLLING PLOTTED FOR COMPARISON

elastohydrodynamic rolling was approximately twice the width after 10^6 cycles of reciprocating, slow speed, dry rolling. The depth of dislocation propagation was also correspondingly greater. The hardness after 10^6 cycles was approximately the same in both cases. No spalls were observed after 10^6 cycles of elastohydrodynamic rolling.

Elastohydrodynamic Slip Characteristics

The concentration of dislocations into bands at early stages of elastohydrodynamic rolling indicates that slip was initiated in a few regions of concentrated stress across the track. Repeated application of stress through the elastohydrodynamic film caused propagation of the dislocations in the bands from the initially slipped regions. The resulting strain caused depressions in the surface that were comparable to the elastohydrodynamic film thickness. While such depressions could result in better ball-track conformity and thicker elastohydrodynamic films, the concentration of slip into narrow bands probably perturbed the film. Stress concentrations at the edges of the bands would produce cross slip and propagation of dislocations into the undeformed areas of the track.

The elimination of surface dislocation sources by elastohydrodynamic oil films that prevent intimate ball-MgO contact probably causes the concentration of slip into bands. Without the film, sufficient solid surface contact exists to generate dislocations across the track as well as at subsurface areas of maximum shear stress. Under elastohydrodynamic conditions, the dislocation sources are limited to existing random dislocations in subsurface areas of maximum shear stress. Propagation of dislocations from such areas results in a limited number of active slip planes that intersect the surface in bands. Similar banding effects have been observed in tensile-test experiments with single-crystal MgO.

Previous measurements of the variation of slip depth with rolling velocity showed that the slip depth decreased at increasing rolling velocities.[2] The maximum rolling velocity used was 2.5 in./sec (6.35 cm/sec). However, the measured track width and slip depth with the much higher elastohydrodynamic-rolling velocities of over 100 in./sec (254 cm/sec) were greater than measured under any conditions of low-velocity rolling. While changes in slip properties related to the presence of the elastohydrodynamic oil film could be causing this effect, wide differences in experimental conditions are also a factor. The elastohydrodynamic-rolling experiments were unidirectional rather than reciprocating. Possible dislocation interactions resulting from the stress field moving alternatively in opposite directions were therefore eliminated. Dislocations on any given set of planes would be less hindered in moving deeper into the crystal. Also, the drill-press apparatus used for the elastohydrodynamic experiments was much more prone to vibration than the low-speed-reciprocating apparatus. The resulting load would tend to vary and could be shocking the MgO crystal. Such conditions of impact would cause much deeper dislocation penetration. The identical track hardness after extended rolling under both conditions indicates that the dislocation density reaches the same, and probably maximum, level.

CONCLUSIONS

The following is a summary of conclusions obtained from this study:

(1) Hardness measurements on tracks produced by reciprocating rolling show the same variation with the number of rolling-contact cycles as track width. Track-width measurements are therefore a measure of dislocation density and extent of interaction in the same manner as hardness.

(2) Transmission electron microscopy has confirmed that the variation in track width and hardness with number of rolling-contact cycles is a direct result of changes in dislocation density and interaction.

(3) The depth of slip remains smaller with higher rolling velocities at extended rolling-contact-cycle levels for low-speed-reciprocating-rolling conditions.

(4) The presence of toluene adsorbed on the MgO surface causes the same change in slip mode and premature spalling as oil, which demonstrates the importance of adsorbed species to rolling-contact slip characteristics for MgO.

(5) Rolling under elastohydrodynamic conditions causes slip to occur in narrow bands across the track. As rolling continues, the bands widen and eventually merge to form a uniform dislocation configuration across the track.

(6) The track width and hardness increase to maximum levels more rapidly under elastohydrodynamic-rolling conditions. The track width after 10^6 rolling-contact cycles is twice that with low-speed-reciprocating rolling, but the track hardness is the same for both conditions of rolling.

While these conclusions were derived from experiments with MgO single crystals, extending them to real rolling-element bearings is of interest. Since fatigue spalls occurred only after a maximum hardness level was attained in the tracks, fatigue spalls caused by dislocation interactions in real bearing materials should not occur until dislocation density and interaction (assumed to be the cause of hardness increases) is sufficiently high. Fatigue cracks occurring before this level is obtained would presumably result from such perturbations as second-phase particles and grain boundaries. Even in this case, the role of the perturbations may be to increase the dislocation density and interactions sufficiently on a local basis to cause fatigue spalling. The Rebinder effect, so dramatically demonstrated with MgO, may also be prevalent in rolling-element bearings in a more subtle form. The influence of surface-active fluids on plastic properties of single-crystal metals was contained in Rebinder's original work. Since the effect was seen only with low-speed-reciprocating rolling in MgO, it may be important only in bearings operating under very thin film conditions produced by high loads and/or slow speeds. However, a knowledge of the nature of the surface interaction would be

required to predict the operating conditions leading to an adverse slip mode and associated spalling. The influence of oxide films on the metal surface may also be important.

RECOMMENDED FUTURE STUDIES

The results of this study have identified several areas worthy of further investigation on the effect of rolling-contact stress on basic deformation and fatigue mechanisms. A detailed analysis of dislocation interactions in MgO should be made by thin-film transmission electron microscopy. Thin films should be prepared at controlled depths beneath the surface to reveal possible variances in dislocation configurations with depth in the track. Identical studies should be made with reciprocating and elastohydrodynamic rolling to determine the effect of different rolling conditions. The dislocation interactions responsible for fatigue failure should be carefully studied by examining specimens prepared from tracks with fatigue spalls. The random nature of fatigue nucleation would require an extensive number of thin films to ensure locating an embryo fatigue crack.

The importance of adsorbed fluids to rolling-contact deformation characteristics of MgO was clearly demonstrated in this study. A further study of the interaction of fluids, ball, and crystal surface is required to determine the extent of this Rebinder effect on other bearing materials. The results would permit a prediction of its importance on fatigue life of metallic rolling-element bearings.

The elastohydrodynamic rolling studies should also be continued to include different fluid types, viscosities, and additives. The effect of these variables and ball load and rolling velocity on dislocation interactions that lead to fatigue spalling should further the understanding of the basic mechanisms responsible for fatigue failures.

With an understanding of the basic rolling-contact deformation and fatigue mechanisms in MgO, similar studies should be performed on more complicated materials that have additional slip systems, second phases, and grain boundaries. Materials chosen for such studies require a sufficiently high yield strength to withstand high rolling-contact stresses without excessive plastic deformation. The proven usefulness of etch-pit techniques in analyzing dislocation configurations resulting from rolling-contact deformation makes established etch-pit techniques on additional desirable feature. Possible materials include silicon-iron and semiconductor single crystals and polycrystals. When the influence of additional factors of multiple slip systems, grain boundaries, surface activity, and second-phase particles is determined, the basic fatigue mechanisms in actual bearing materials should be analyzed.

REFERENCES

(1) Amateau, M. F., and Spretnak, J. W., "Plastic Deformation of Magnesium Oxide Crystals Subjected to Rolling-Contact Stresses", Journal of Applied Physics, 34 (8), 2340-2345 (August, 1963)

(2) Dufrane, K. F., and Glaeser, W. A., "Study of Rolling-Contact Phenomena in Magnesium Oxide", NASA Contract No. NAS 3-6263, September 25, 1967.

(3) Westbrook, J. H., and Jorgensen, P. J., "Indentation Creep of Solids", Met. Soc. AIME, Trans., 233, 425 (February, 1965).

(4) Westwood, A.R.C., Goldheim, D. L., and Lye, R. G., "Rebinder Effects in MgO", RIAS TR 67-6, NONR-4162(00), June, 1967.

(5) Westwood, A.R.C., "Effects of Adsorption on Hardness and Mobility of Near-Surface Dislocations in Non-Metals", RIAS TR 66-6, NONR-4162(00), August, 1966.

(6) Westwood, A.R.C., Goldheim, D. L., and Lye, R. G., "Further Observations on Rebinder Effects in MgO", November, 1967, to be published.

(7) Grubin, A. N., and Vinogradova, I. E., "Investigation of the Contact of Machine Components", Moscow, Ts NIITMASH, Book No. 30 (1949), (D.S.I.R., London, Translation No. 337).

(8) Kannel, J. W., Bell, J. C., Walowit, J. A., and Allen, C. M., "A Study of the Influence of Lubricant on High-Speed Rolling-Contact Bearing Performance", ASD-TDR-61-643, Part VII, Wright-Patterson AFB, Ohio (1967).

KFD:WAG/dc

DISTRIBUTION LIST

	Copies
NASA Headquarters Washington, D. C. 20546 Attention: N. F. Rekos (RAP)	1
M. Comberiate	1
NASA-Lewis Research Center 21000 Brookpark Road Cleveland, Ohio 44135 Attention: John H. DeFord, M.S. 60-5	1
Technology Utilization Office	1
P. T. Hacker, M. S. 5-3	1
I. I. Pinkel, M. S. 5-3	1
J. Howard Childs, M. S. 60-4	2
D. Townsend, M. S. 60-4	4
L. Macioce, M. S. 60-4	1
E. E. Bisson, M. S. 5-3	1
R. L. Johnson, M. S. 23-2	1
W. J. Anderson, M. S. 23-2	1
E. V. Zaretsky, M. S. 6-1	12
Reports Control Office, M. S. 5-5	1
FAA Headquarters 800 Independence Avenue, S. W. Washington, D. C. 20553 Attention: F. B. Howard/SS-120	1
Brig. General J. C. Maxwell	1
Air Force Materials Laboratory Wright-Patterson AFB, Ohio 45433 Attention: MANL	1
R. Adamczak & F. Harsacky	1
MAMD	1
Walter Trapp	1
NASA-Langley Research Center Langley Station Hampton, Virginia 23365 Attention: Mark R. Nichols	1
United Aircraft Corporation Pratt & Whitney Aircraft Division East Hartford, Connecticut 06108 Attention: R. P. Schevchenko	1
P. Brown	1
General Electric Company Gas Turbine Division Evendale, Ohio 45215 Attention: B. Venable	1
E. N. Bamberger	1
California Research Corporation Richmond, California 94802 Attention: Douglas Godfrey	1
Dow Chemical Company Abbott Road Buildings Midland, Michigan 48640 Attention: Dr. R. Gunderson	1
Crucible Steel Company of America The Oliver Building Mellon Square Pittsburgh, Pennsylvania 15222	1
Dow Corning Corporation Midland, Michigan 48640 Attention: R. W. Awe & H. M. Schiefer	1
Allegheny Ludlum Steel Corporation Oliver Building Pittsburgh, Pennsylvania 15222	1
Mechanical Technology, Incorporated Latham, New York 14603 Attention: B. Sternlicht	1
Director Government Research Laboratory Esso Research & Engineering Company P. O. Box 8 Linden, New Jersey 07036	1
Industrial Tectonics, Inc. Research & Development Division 18301 Santa Fe Avenue Compton, California 90220 Attention: Heinz Hanau	1
Monsanto Research Corporation Everett Station Boston, Massachusetts 02109 Attention: Dr. John O. Smith	1
Pennsylvania State University Department of Chemical Engineering University Park, Pennsylvania 16801 Attention: Dr. E. E. Klause	1
Fafnir Bearing Company 37 Booth Street New Britian, Connecticut 06051 Attention: H. B. Van Dorn	1
General Electric Company General Engineering Laboratory Schenectady, New York 12305	1

DISTRIBUTION LIST (Continued)

	Copies
Borg-Warner Corporation Roy C. Ingersoll Research Center Wolf and Algonquin Roads Des Plaines, Illinois 60016	1
General Motors Corporation New Departure Division Bristol, Connecticut 06010 Attention: W. O'Rourke	1
Franklin Institute Labs 20th and Parkway Philadelphia, Pennsylvania 19133 Attention: Otto Decker	1
Westinghouse Electric Corporation Research Laboratories Beulah Road, Churchill Borough Pittsburgh, Pennsylvania 15235 Attention: John Boyd	1
Midwest Research Institute 425 Volker Boulevard Kansas City, Missouri 64110 Attention: V. Hopkins & A. D. St. John	1
Socony Mobil Oil Company Research Department Paulsboro Laboratory Paulsboro, New Jersey 08066 Attention: Ed. Oberright	1
The Marlin-Rockwell Corporation Jamestown, New York 14701 Attention: Arthur S. Irwin	1
Southwest Research Institute San Antonio, Texas 78205 Attention: P. M. Ku	1
IIT Research Institute West 35th Street Chicago, Illinois 60616 Attention: Warren Jamison	1
NASA-Lewis Research Center 21000 Brookpark Road Cleveland, Ohio 44135 Attention: Library	1
Sinclair Research, Incorporated 400 E. Sibley Boulevard Harvey, Illinois 60426 Attention: M. R. Fairlie Director of Products Division	1
General Electric Company Research and Development Center P. O. Box 8 Schenectady, New York 12301 Attention: Dr. J. H. Westbrook	1
NASA-Scientific and Technical Information Facility Box 5700 College Park, Maryland 20740 Attention: NASA Representative	6
AiResearch Manufacturing Company Dept. 93-3 9851 Sepulveda Boulevard Los Angeles, California 90009 Attention: Hans. J. Poulsen	1
Department of the Army U. S. Army Aviation Material Labs. Fort Eutis, Virginia 23604 Attention: J. W. White Propulsion Division	1
SKF Industries, Inc. Engineering & Research Center 1100 First Avenue King of Prussia, Pennsylvania 19104 Attention: L. B. Sibley T. Tallian	1 1
Nyatt Division New Departure Bearing Company Sandusky, Ohio 44870 Attention: B. Ruley	1
Timkin Roller Bearing Company Canton, Ohio 44701 Attention: Dr. W. Littmann	1
Caterpillar Tractor Peoria, Illinois 61601 Attention: B. Kelley	1
General Motors Research Laboratory Warren, Michigan 48089 Attention: Nils L. Buench	1
Department of the Navy Naval Ship Research Development Center Annapolis, Maryland 21402 Attention: Paul Schatzberg	1
University of Arizona College of Mines Tucson, Arizona 85721 Attention: Dr. L. J. Demer	1
Martin Marietta Corporation Research Institute for Advanced Studies Baltimore, Maryland 21227 Attention: Dr. A.R.C. Westwood	1